

PCCP

Accepted Manuscript



This is an *Accepted Manuscript*, which has been through the Royal Society of Chemistry peer review process and has been accepted for publication.

Accepted Manuscripts are published online shortly after acceptance, before technical editing, formatting and proof reading. Using this free service, authors can make their results available to the community, in citable form, before we publish the edited article. We will replace this *Accepted Manuscript* with the edited and formatted *Advance Article* as soon as it is available.

You can find more information about *Accepted Manuscripts* in the [Information for Authors](#).

Please note that technical editing may introduce minor changes to the text and/or graphics, which may alter content. The journal's standard [Terms & Conditions](#) and the [Ethical guidelines](#) still apply. In no event shall the Royal Society of Chemistry be held responsible for any errors or omissions in this *Accepted Manuscript* or any consequences arising from the use of any information it contains.

Extracting Biomolecule Collision Cross Sections from the High-resolution FT-ICR Mass Spectral Linewidths

Ting Jiang,¹ Yu Chen,² Lu Mao,¹ Alan G. Marshall^{3,4*} and Wei Xu^{1*}

¹School of Life Science, Beijing Institute of Technology, Beijing 100081, China

²The Roy J. Carver Biotechnology Center, University of Illinois at Urbana-Champaign, Urbana, IL 61801, USA

³ Ion Cyclotron Resonance Program, National High Magnetic Field Laboratory, Florida State University, Tallahassee, FL, 32310

⁴Department of Chemistry and Biochemistry, Florida State University, Tallahassee, FL, 32306

*Corresponding Authors:

Wei Xu School of Life Science Beijing Institute of Technology Haidian, Beijing, 100081, China Email: weixu@bit.edu.cn Web: http://www.escience.cn/people/weixu	Alan G. Marshall Ion Cyclotron Resonance Program National High Magnetic Field Laboratory Tallahassee, Florida 32310, USA Email: marshall@magnet.fsu.edu
---	--

Abstract:

It is known that ion collision cross section (CCS) may be calculated from the linewidth of a Fourier transform ion cyclotron resonance (FT-ICR) mass spectral peak at elevated pressure (e.g., $\sim 10^{-6}$ Torr). However, the high mass resolution of FT-ICR is sacrificed in those experiments due to the high buffer gas pressure. In this study, we describe a linewidth correction method to eliminate the windowing-induced peak broadening effect. Together with the energetic ion-neutral collision model previously developed by our group, this method enables the extraction of CCSs of biomolecules from high-resolution FT-ICR mass spectral linewidths, obtained at typical operating buffer gas pressure of modern FT-ICR instruments ($\sim 10^{-10}$ Torr). CCS values for peptides including MRFA, angiotensin I, and bradykinin measured by the proposed method agree well with ion mobility measurements, and the unfolding of protein ions (ubiquitin) at higher charge states is also observed.

Introduction:

Structural analysis of a biomolecule, such as the conformations of a protein, is critically important to understand its biological functions at a molecular level.^{1,2} Mass spectrometry (MS) has been widely employed for biomolecule identification, quantitation, and structure determination.³ Based on different principles, ion mobility spectrometry (IMS) and tandem mass spectrometry (tandem MS) are two widely used mass spectrometric techniques to acquire complementary ion structural information of an ion.⁴⁻⁶ With the rapid development of proteomics, there is increasing demand for complementary ion structure determination techniques.

Efforts have been made to perform ion CCS measurements with mass analyzers, so that molecular weight, fragmentation pattern, and CCS of an ion could be obtained simultaneously in a single device. Since the 1960's, a number of experiments have been carried out to measure CCSs of low-mass ions in an ion cyclotron resonance (ICR) cell at elevated pressures (up to a few mTorr).⁷⁻¹⁰ For example, CCS measurements for crown ether ions have been demonstrated from FT-ICR MS at elevated pressures.¹¹ In the elevated pressure range ($> \sim 10^{-6}$ Torr), ion motion decay is sufficiently fast to determine ion CCSs from frequency domain linewidths in FT-ICR mass spectra. In 2014, a method for ion CCS measurements in quadrupole ion traps was also proposed theoretically, based on a time-frequency analysis method.¹²

We recently reported a CCS measurement method based on time-domain data acquired by FT-ICR mass spectrometry.¹³ Here, we present a method in which the corrected linewidths of FT-ICR mass spectra in frequency domain are used to determine CCSs of biomolecules. In this work, ion motion-induced image currents were recorded in the typical working pressure range of modern FT-ICR cells ($< 10^{-9}$ Torr), in which the region windowing-induced peak broadening effect needs to be taken into account to accurately calculate ion CCSs from mass spectral linewidths. Experimental parameters were carefully chosen so that image current decay was pressure-dominant.¹⁴ A linewidth correction method was then developed to eliminate windowing-induced peak broadening effect. While maintaining high MS resolution, we calculated CCSs of MRFA, bradykinin, angiotensin I, and ubiquitin directly from

corrected linewidths in frequency-domain FT-ICR mass spectra. The presently determined CCSs agree well with those measured by ion mobility mass spectrometry (see below), suggesting that the proposed methodology offers a potentially complementary approach to probe biomolecule gas-phase structure. Compared to the time-domain approach,¹³ this frequency-domain linewidth correction method is more straightforward without the need of advanced data processing, and it can be easily extended to other type of high-resolution mass analyzers, such as Orbitraps.^{15,16}

Theory and Methods

To perform CCS measurements inside an FT-ICR cell, a correlation between mass spectra linewidth and ion CCS must be established, assuming that the energetic hard-sphere collision model accurately describes ion-neutral collisions. Details of the collision model are described by D. Guo et al.¹⁷ Briefly, the total number of ions in a coherent packet (N), and corresponding image current signal at cyclotron frequency (I), are described by exponential decay.¹⁴

$$N(t) \sim e^{-t/\tau}, \quad I(t) \sim e^{-t/\tau} \cos(\omega t) \quad (1)$$

τ is an exponential damping time constant equal to $1/nv\sigma$, in which n is the neutral density ($n=P/KT'$ for an ideal gas, P is pressure, K is Boltzmann constant, and T' is temperature), v is ion speed, and σ is the ion CCS. After Fourier transformation of Eqn. (1), the real part corresponds to the absorption-mode line shape ($A(\omega)$),

$$A(\omega) = \frac{A_0}{1 + [(\omega - \omega_0) \frac{1}{\sigma n v}]^2} \quad (2)$$

in which A_0 is the amplitude and ω_0 is the ion cyclotron frequency. Thus,

$$\sigma = \frac{\Delta\omega}{2nv} \quad (3)$$

$\Delta\omega$ in Eqn. (3) is the peak width of an image current with infinite time-domain transient length. In practice, the time-domain transient duration is limited by factors such as data storage memory size, duty cycle (e.g., for on-line liquid chromatography/MS), data analysis speed, etc.. As shown in Figure 1 (a-d), limited transient length causes frequency-domain peak broadening (windowing effect) following fast Fourier transform (FFT)^{18, 19}. Various types of truncation window

functions have been applied to minimize windowing effects.^{20, 21} In order to extrapolate ion CCSs from linewidth, windowing effects need to be corrected, especially when high-resolution mass spectra and CCSs are acquired simultaneously. In that case, pressure-induced ion motion decay is slow, and peak broadening caused by windowing effects can be comparable to (or larger than) that induced by ion-neutral collisions.

Windowing-induced peak broadening compensated for rectangular windows of different window widths. For an exponential decay signal truncated by a rectangular window of width, T , the real component Fourier transform frequency-domain spectrum is:

$$\int_0^T e^{-t/\tau} \cos(\omega t) dt = \frac{e^{-T/\tau} \tau (e^{T/\tau} - \cos(T\omega) + \tau \omega \sin(T\omega))}{1 + \tau^2 \omega^2} \quad (4)$$

Before correction, the measured linewidth at half maximum ($\Delta\omega'$) can be used to calculate the decay time constant,

$$\frac{e^{-T/\tau} \tau (e^{T/\tau} - \cos(T\Delta\omega') + \tau \Delta\omega' \sin(T\Delta\omega'))}{1 + \tau^2 (\Delta\omega')^2} = \frac{e^{-T/\tau} \tau (e^{T/\tau} - 1)}{2} \quad (5)$$

Experimentally, $\Delta\omega'$ could be measured directly from the absorption-mode spectrum, and T , the rectangular window width. Eqn. (5) may be solved numerically to obtain the decay time constant, τ , from the corrected absorption-mode linewidth ($\Delta\omega = 2/\tau$), as shown in Eqn. (5). Based on Eqn. (5), Figure 1e shows the correlation between the measured linewidths ($\Delta\omega'$) and corrected linewidths ($\Delta\omega$) processed by different square window widths. It should be noticed that improved agreement between measured and corrected linewidths is observed for 1) longer transient data; or 2) higher buffer gas pressure, which leads to faster decay and thus larger corrected linewidth.

Experimental Section

Experiments were performed with a custom-built 9.4 T FT-ICR mass spectrometer with cell pressure 10^{-10} Torr (unless otherwise specified).²² Ultramark, bradykinin, angiotensin I, ubiquitin, and cytochrome *c* were purchased from Sigma Aldrich (St. Louis, MO, USA). Samples were used without further purification.

Electrosprayed samples were diluted to 1.0 $\mu\text{mol/L}$ in methanol/water 1:1 v/v with 0.1% formic acid. Image current data were collected for 6.115 s transient with 8388608 data points. Data were further processed with Matlab (MathWorks Inc.) without zero-filling.

Results and Discussion

To accurately measure the CCS of an ion in a FT-ICR cell, ion motion decay must be pressure-dominant. In other words, the mass spectral peak width needs to be determined by ion-neutral collisions. Other factors, including electric and magnetic field inhomogeneity, space charge effects, and spectral leakage due to windowing also affect the linewidth and peak shape in an FT-ICR mass spectrum. Besides the use of corrected linewidth to eliminate the windowing effect, experimental setup and instrument parameters were carefully controlled to minimize field inhomogeneity and space charge effects.

Ideally, the three-dimensional electrostatic trapping potential in an ICR cell should be perfectly quadrupolar. However, higher-order fields contributions are inevitable due to electrode geometry, electrode truncation, fabrication deviation, etc.²³ It is known that the effect of higher-order electric fields components increases with increasing ion cyclotron post-excitation radius. We used two methods to minimize electric field imperfection: 1) an ICR cell with minimum higher-order field components was employed; 2) ions were excited to a relative low cell radius. An electrically compensated ICR cell with an inner diameter (ID) of 94 mm was used.²² Ions were excited to a radius of 18.8 mm (40% cell radius) before detection. To probe the linewidth effects caused by field imperfection, ions were excited to different radii before image current measurement. As shown in Figure 2a, linewidth for ubiquitin (m/z 1071.595) increased slightly from 0.271 to 0.280 Hz (~3.6% variation) as the ion excitation radius varies increased from 14.1 to 28.2 mm. It is also known that the effect of space charge decreases with increasing ion post-excitation cyclotron radius, because ions of different m/z spread out around a wider circumference. Therefore, as a compromise between these two effects, ion excitation radius was kept at 18.8 mm

for all experiments unless otherwise specified. Due to the stronger high-order electric field and image charge forces at higher ion excitation radius,¹⁷ a small shoulder could be observed for the mass spectral peak at excitation radius of 28.2 mm.

Coulomb interactions between ions cause dephasing of ion coherence, which leads to peak broadening.^{24, 25} Space charge effects were minimized by limiting the total ion number in the ICR cell. Thus, ions were accumulated for 40 ms in an external octopole accumulator before injection into the cell. To characterize space charge effects, broadband mass spectra and SWIFT²⁰-isolated precursor mass spectra were both collected and their linewidths compared (see Figure 2b). The detected peak widths for the broadband and SWIFT-isolated spectra are similar for MRFA, angiotensin I, and ubiquitin, suggesting that space charge effects are negligible.

Buffer gas pressure inside the ICR cell was controlled by a pulsed leak valve, and multiple experiments were carried out to confirm the prerequisite. In Figures 2c and 2d, the corrected linewidths for ubiquitin and MRFA is plotted as a function of buffer gas pressures. Nearly linear relationships are observed for all cases. In addition, intersection points with the y -axis are close to zero (within -0.016 to -0.01 Hz), indicating that the corrected linewidth is indeed pressure-dominant. Furthermore, mass spectral peaks for ubiquitin disappear on buffer gas pressure was increased from 10^{-10} to 10^{-9} Torr, indicating that ion-neutral collisions are overwhelming and ubiquitin ions are totally dephased and/or ion packet coherence is destroyed during the 6.115 s image current detection duration (see Figure 3).

Under carefully controlled experimental conditions, the corrected linewidths were used to calculate the CCSs for different ions. Figure 4a shows the calculated CCSs for ubiquitin ions of different charge states. In the experiments, isotope ions were assumed to exhibit identical CCS. CCSs calculated for different buffer gas pressures (10^{-10} , 2.3×10^{-10} , 5.2×10^{-10} and 10^{-9} Torr) and repeated measurements (3 repeated measurements at 10^{-10} Torr) were processed together. Previous experiments have shown that ubiquitin exhibits a more extended conformation as more charges are added, based on analytical techniques such as electron capture dissociation (ECD)^{4, 26, 27}, H/D exchange²⁸ and IMS-MS.^{29, 30} Two effects may account for the relatively

large error bars in CCS measurements: (a) unfolding of an ion, especially for a large biomolecular ion, could be a continuous process, so that the structure and CCS of an ion would span a range instead of several fixed values;³¹ and (b) differences between parallel experiments, such as exact ion number, statistical nature of ion-neutral collisions, variation of temperature, buffer gas pressure inside the FT-ICR cell, etc. Figure 4b shows the correlation between the CCSs of MRFA, bradykinin, angiotensin I, and ubiquitin measured in the present study and those determined by IMS experiments. An excellent linear relationship was observed, suggesting that the present method could serve as a complementary approach compared to IMS for ion structure analysis. Moreover, because the CCS measurements were performed at low buffer gas pressures ($<10^{-9}$ Torr), high resolution mass spectra could be obtained simultaneously. As seen in Figures 4c to 4e, a resolving power of $\sim 500,000$ (at m/z 1600) or higher (at m/z 433 and m/z 531) was achieved at 10^{-10} Torr.

Conclusions:

As a proof-of-principle, we have determined ion CCSs from the corrected linewidths of FT-ICR mass spectral peaks. Under controlled experimental conditions, high resolution mass spectra acquisition and CCS measurements could be performed at the same time at a relatively low buffer gas pressure ($<10^{-9}$ Torr). Because the maximum exchange energy that an ion could obtain from an ion-neutral collision is inversely proportional to the square of m/z ,¹⁷ more collisions are required for sufficient damping for larger ions. The present method appears suitable for ions smaller than ubiquitin, except for very rigid ions with fragmentation energy higher than that for ubiquitin ions. Larger ICR cells and stronger magnetic fields are required in order to extend ion mass range for CSS measurements.

Acknowledgements

This work was supported by NNSF of China (21205005, 21475010), 1000 plan (China), MOST Instrumentation Program (China) (2011YQ0900502), NSF (DMR-11-57490, CHM-1019193) and the State of Florida.

References:

1. C. Branden and J. Tooze, *Introduction to protein structure*, Garland New York, 1991.
2. A. Nicholls, K. A. Sharp and B. Honig, *Proteins: Structure, Function, and Bioinformatics*, 1991, 11, 281-296.
3. B. Domon and R. Aebersold, *science*, 2006, 312, 212-217.
4. K. Breuker, H. Oh, D. M. Horn, B. A. Cerda and F. W. McLafferty, *Journal of the American Chemical Society*, 2002, 124, 6407-6420.
5. K. B. Shelimov, D. E. Clemmer, R. R. Hudgins and M. F. Jarrold, *Journal of the American Chemical Society*, 1997, 119, 2240-2248.
6. R. Aebersold and M. Mann, *Nature*, 2003, 422, 198-207.
7. D. Wobschall, R. A. Fluegge and J. R. Graham Jr, *The Journal of Chemical Physics*, 1967, 47, 4091.
8. W. T. Huntress Jr, *The Journal of Chemical Physics*, 1971, 55, 2146.
9. P. P. Dymerski and R. C. Dunbar, *The Journal of Chemical Physics*, 1972, 57, 4049-4050.
10. D. P. Ridge and J. L. Beauchamp, *The Journal of Chemical Physics*, 1976, 64, 2735-2746.
11. F. Yang, J. E. Voelkel and D. V. Dearden, *Analytical Chemistry*, 2012, 84, 4851-4857.
12. M. He, D. Guo, Y. Chen, X. Xiong, X. Fang and W. Xu, *Analyst*, 2014, 139, 6144-6153.
13. L. Mao, Y. Chen, Y. Xin, Y. Chen, L. Zheng, N. K. Kaiser, A. G. Marshall and W. Xu, *Analytical chemistry*, 2015, 87, 4072-4075.
14. A. G. Marshall, M. B. Comisarow and G. r. Parisod, *The Journal of Chemical Physics*, 1979, 71, 4434.
15. Q. Hu, R. J. Noll, H. Li, A. Makarov, M. Hardman and R. Graham Cooks, *Journal of Mass Spectrometry*, 2005, 40, 430-443.
16. W. Xu, J. B. Maas, F. J. Boudreau, W. J. Chappell and Z. Ouyang, *Analytical Chemistry*, 2011, 83, 685-689.
17. D. Guo, Y. Xin, D. Li and W. Xu, *Physical Chemistry Chemical Physics*, 2015, 17, 9060-9067.
18. J. W. Cooley and J. W. Tukey, *Mathematics of computation*, 1965, 19, 297-301.
19. F. R. Verdun, C. Giancaspro and A. G. Marshall, *Applied spectroscopy*, 1988, 42, 715-721.
20. A. G. Marshall, T. C. L. Wang and T. L. Ricca, *Journal of the American Chemical Society*, 1985, 107, 7893-7897.
21. H. S. Kim and A. G. Marshall, *Journal of Mass Spectrometry*, 1995, 30, 1237-1244.
22. N. K. Kaiser, J. J. Savory, A. M. McKenna, J. P. Quinn, C. L. Hendrickson and A. G. Marshall, *Analytical Chemistry*, 2011, 83, 6907-6910.
23. M. L. Easterling, T. H. Mize and I. J. Amster, *Analytical chemistry*, 1999, 71, 624-632.
24. S.-J. Han and S. K. Shin, *Journal of the American Society for Mass Spectrometry*, 1997, 8, 319-326.
25. C. L. Hendrickson, S. C. Beu and D. A. Laude, *Journal of the American Society for Mass Spectrometry*, 1993, 4, 909-916.
26. D. M. Horn, K. Breuker, A. J. Frank and F. W. McLafferty, *Journal of the American Chemical Society*, 2001, 123, 9792-9799.
27. E. W. Robinson, R. D. Leib and E. R. Williams, *Journal of the American Society for Mass Spectrometry*, 2006, 17, 1470-1480.
28. M. A. Freitas, C. L. Hendrickson, M. R. Emmett and A. G. Marshall, *International Journal of Mass Spectrometry*, 1999, 185-187, 565-575.

29. E. R. Badman, C. S. Hoaglund-Hyzer and D. E. Clemmer, *Journal of the American Society for Mass Spectrometry*, 2002, 13, 719-723.
30. C. S. Hoaglund, S. J. Valentine, C. R. Sporleder, J. P. Reilly and D. E. Clemmer, *Analytical Chemistry*, 1998, 70, 2236-2242.
31. S.-H. Chen and D. Russell, *Journal of The American Society for Mass Spectrometry*, 2015, DOI: 10.1007/s13361-015-1191-1, 1-11.

Figure 1

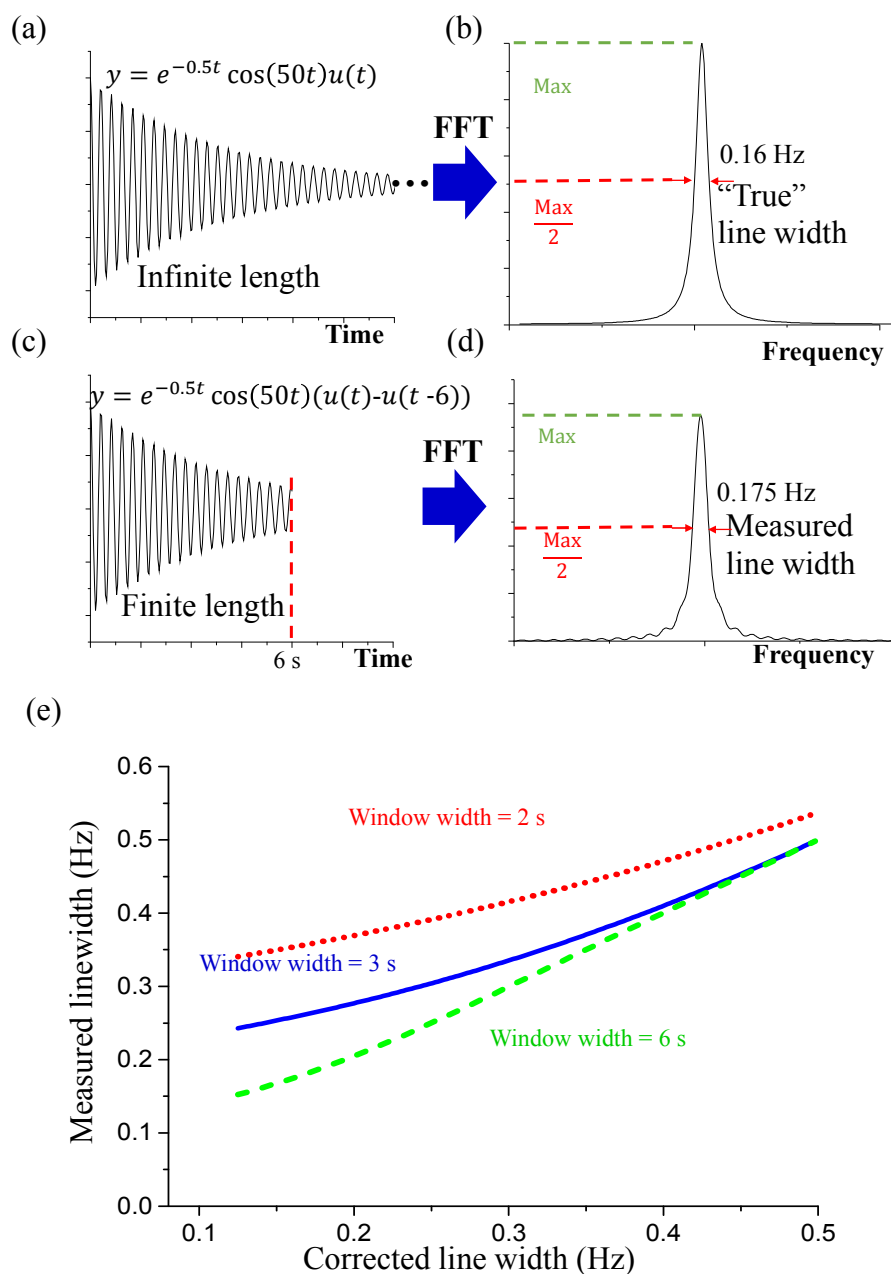


Figure 1. (a) An infinitely long time-domain signal. (b) Absorption-mode frequency spectrum of the time-domain signal of (a). (c) The same time-domain signal weighted by a 6-second truncation window. (d) Frequency spectrum of the time-domain signal of (c). (e) Relationship between the detected linewidth and the corrected linewidth.

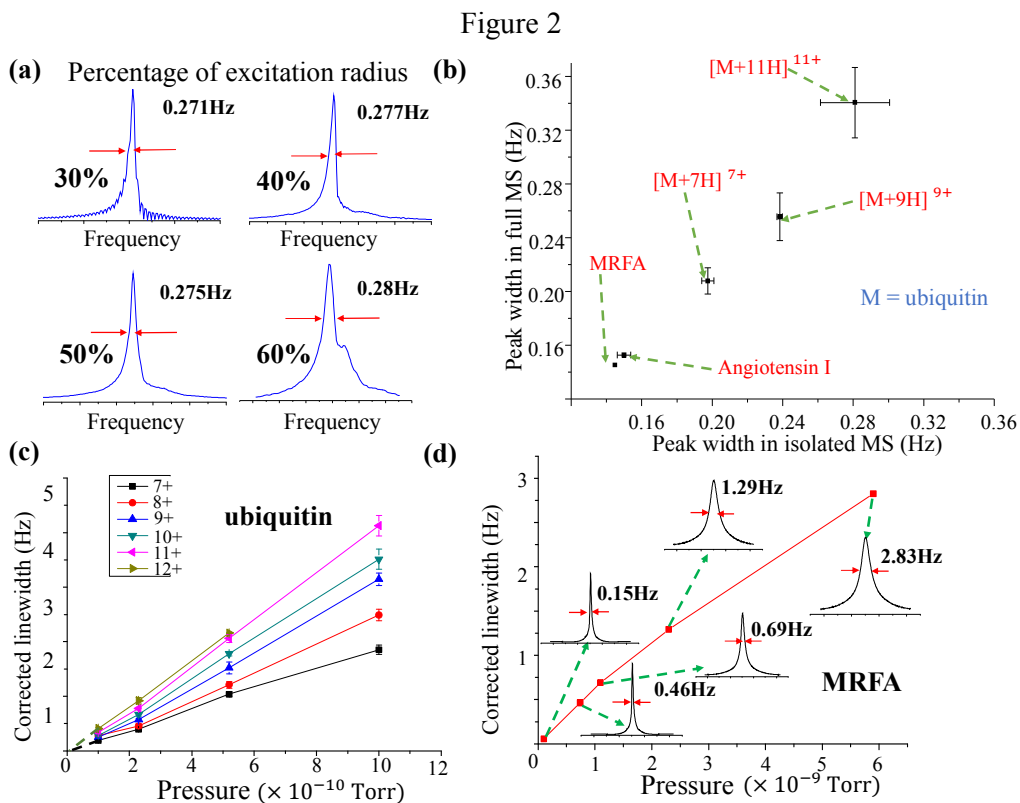


Figure 2. (a) Measured linewidths for ubiquitin ions (m/z 1071.595 Da) at different post-excitation excitation ion cyclotron radii. (b) Measured linewidths in the full mass spectrum without performing ion isolation versus those in the SWIFT-isolated spectrum. (c) Corrected linewidths for ubiquitin ions of different charge states at different buffer gas pressures. (d) Corrected linewidths for MRFA ions at different buffer gas pressures.

Table 1. Linear fitting equations and standard deviations for the lines in Figure 2c.

Charge states	Fitting Equations	R^2
+7	$y=0.18661 x - 0.01625$	0.98458
+8	$y=0.23123 x + 0.04004$	0.97883
+9	$y=0.3071 x - 0.08442$	0.98396
+10	$y=0.35232 x - 0.07839$	0.99522
+11	$y=0.39769 x - 0.12446$	0.97886
+12	$y=0.41693 x - 0.01004$	0.9999

Figure 3

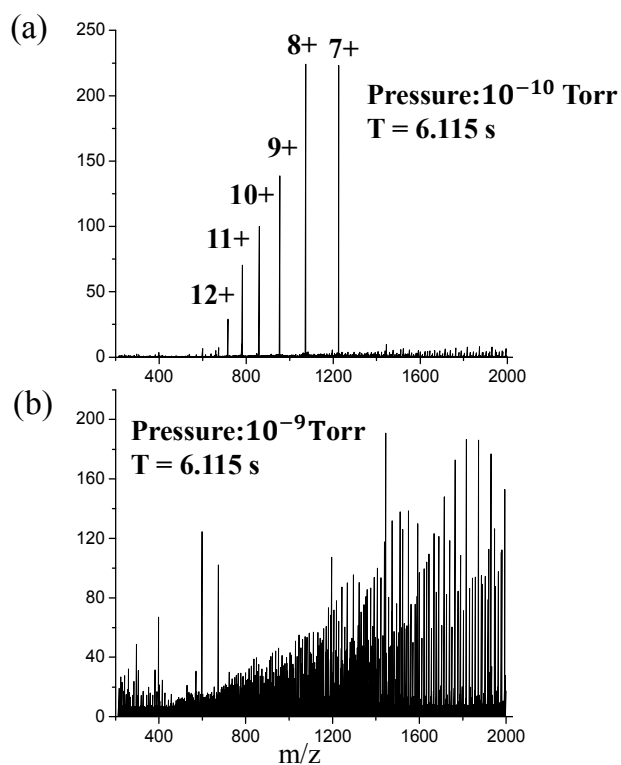


Figure 3. Positive electrospray ionization 9.4 T FT-ICR mass spectra of ubiquitin (a) at base pressure of 10^{-10} Torr; (b) at a pressure of 10^{-9} Torr. Signal-to-noise ratio is greatly reduced in (b) because the time-domain signal damps early in the data acquisition period.

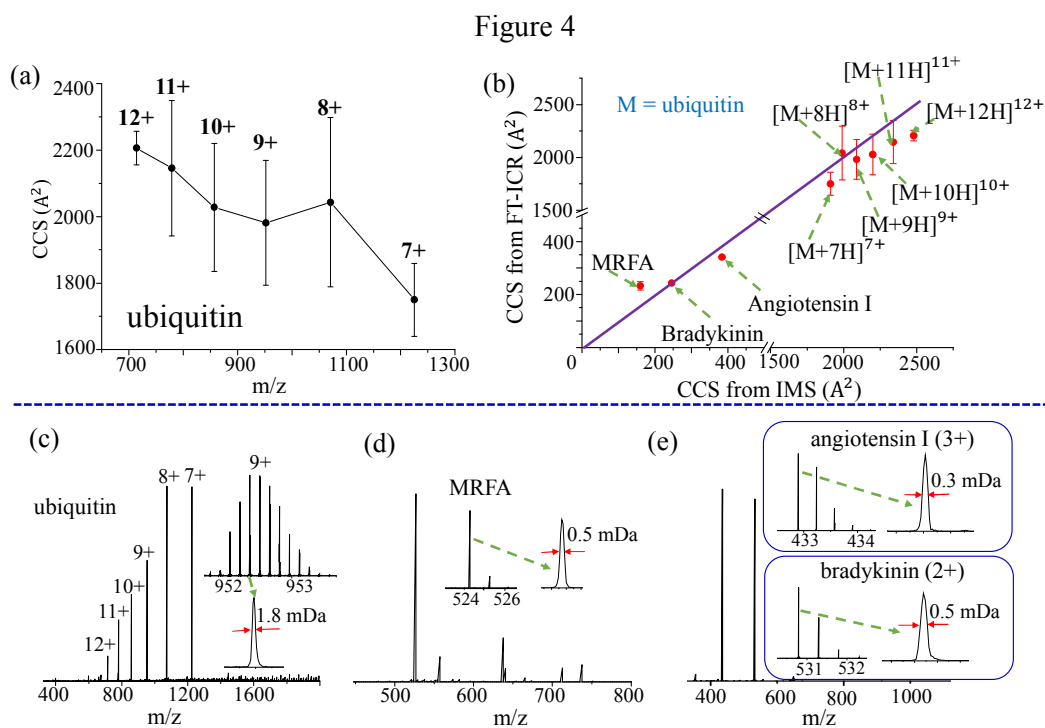


Figure 4. (a) CCSs of ubiquitin ions of different charge states. (Calculated based on results collected at different buffer gas pressures--see text for details.) (b) CCSs obtained in this work versus the results from ion mobility measurements. The corresponding mass spectra of (c) ubiquitin, (d) MRFA, (e) angiotensin I, and bradykinin.

TOC

A linewidth correction method was introduced, which enables the measurement of biomolecule CCSs in FT-ICR cells at 10^{-10} Torr.

